Hindawi Publishing Corporation
Journal of Nanomaterials
Volume 2015, Article ID 192174, 6 pages
http://dx.doi.org/10.1155/2015/192174

Research Article

Co_3O_4 Electrode Prepared by Using Metal-Organic Framework as a Host for Supercapacitors

Jiaqiang Jiang, Fuxiang Wei, Genxi Yu, and Yanwei Sui

School of Materials Science & Engineering, China University of Mining and Technology, Xuzhou, Jiangsu 221008, China

Correspondence should be addressed to Fuxiang Wei; weifuxiang2001@163.com

Received 23 October 2014; Revised 2 March 2015; Accepted 2 March 2015

Academic Editor: Takuya Tsuzuki

Co_3O_4 nanoparticles were prepared from cobalt nitrate that was accommodated in the pores of a metal-organic framework (MOF) ZIF-8 ($Zn(MeIM)_2$, MeIM = 2-methylimidazole) by using a simple liquid-phase method. Analysis by scanning electron microscopy (SEM) and transmission electron microscopy (TEM) showed that the obtained Co_3O_4 was composed of separate nanoparticles with a mean size of 30 nm. The obtained Co_3O_4 nanoparticles exhibited superior electrochemical property. Co_3O_4 electrode exhibited a maximum specific capacitance of 189.1 F g^{-1} at the specific current of 0.2 A g^{-1}. Meanwhile, the Co_3O_4 electrode possessed the high specific capacitance retention ratio at the current density ranging from 0.2 to 1.0 A g^{-1}, thereby indicating that Co_3O_4 electrode suited high-rate charge/discharge.

1. Introduction

Supercapacitor has gained great interests from many researchers with fast charging rate, high power density, and long service life, which is widely applied to portable apparatus, data memory storage system, electric vehicle power supply, and emergency back-up power supply [1–3]. In particular, it has great advantage in the electric vehicle. The United States, Japan, Russia, and so forth have successively invested plenty of manpower and material to research and develop it. The supercapacitor electrode mainly includes three kinds of materials: carbon materials, transition metal oxides, and conductive polymers [4–6]. Co_3O_4 belongs to cheap metallic oxide in all transition metal oxides, which has been frequently used as the supercapacitor electrode for many years due to good electrochemical capacitance property thereof. However, Co_3O_4 nanoparticles have sufficiently small particle size; thereby its activity is greatly enhanced as electrode material, and the specific capacitance is effectively increased [7–9]. Currently, some methods of preparing the Co_3O_4 nanoparticles have been reported in a lot of literatures, and many Co_3O_4 nanoparticles with the small particle size have been introduced [10–12]. However, it is urgent to prepare Co_3O_4 nanoparticles with smaller particle size and better dispersion with continuous technology innovation and production demand [12].

Metal-organic frameworks (MOFs) have been widely noticed by people due to open pores, steady pore structures, excellent heat stability, and high ordered crystalline state as new porous materials. They become a new trend to the research fields, such as gas separation and preservation, sensors, drug delivery, and heterogeneous catalysis [13–16]. Bhakta et al. demonstrated that MOFs could be employed as effective hosts for nanoscale metal hydride such as $NaAlH_4$ recently [17]. Fischer et al. were the first to show that MOFs could be used as hosts for transition metal oxides nanoclusters (e.g., TiO_2 and ZnO) by gas-phase infiltration with organometallic precursors [18, 19]. The ZIF-8 framework ($Zn(MeIM)_2$, MeIM = 2-methylimidazole), one of the representative MOFs, holds an intersecting three-dimensional channel system, a large pore size (11.6 Å in diameter), and high thermal stability (in N_2) as well as good chemical resistance to water and organic solvents [20–23], which may be an appropriate host for preparing Co_3O_4 nanoparticles by using a solution-based method to introduce the cobalt precursor.

Herein, we report the example of adopting ZIF-8 as host for preparing Co_3O_4 nanoparticles by a facile liquid-phase

method. We show that the directness of cobalt nitrate accommodated in the pores of a ZIF-8 yields Co_3O_4 nanoparticles after removing the ZIFs. For comparison, we simultaneously analyze the method for preparing Co_3O_4 nanoparticles by using thermal decomposition via ZIF-67 and compare the structures and the electrochemical property.

2. Experimental

2.1. Synthesis. ZIF-67 ($Co(MeIM)_2$, MeIM = 2-methylimidazole) was prepared according to the reported procedures [24]. Co_3O_4 nanoparticles were synthesized by heating ZIF-67 at a temperature of 600°C for 5 hours with a heating rate of 2°C/min in air (the prepared Co_3O_4 nanoparticles were denoted as Co_3O_4-TH).

ZIF-8 was prepared according to a previously published procedure [21]. Then, the Co_3O_4 nanoparticles were prepared by soaking cobalt nitrate hexahydrate into the ZIF-8 pore, including the following steps: weighting 0.5 g of ZIF-8, decentralizing them into 10 mL of absolute ethyl alcohol where 0.6 g $Co(NO_3)_2 \cdot 6H_2O$ is dissolved, stirring for 2 hours by a magnetic stirrer at the ambient temperature, washing the prepared powder three or four times by ethyl alcohol and deionized water, heating up the prepared compound to 600°C at the heating rate of 2°C/min and keeping for 5 hours, decentralizing the prepared powder into NH_4Cl (5 M)-$NH_3 \cdot H_2O$ (2.5 M) aqueous solution to remove ZnO decomposed by ZIF-8, centrifugally cleaning and collecting prepared black Co_3O_4, and then placing them into an oven at 100°C to dry for 12 hours (the prepared Co_3O_4 nanoparticles were denoted as Co_3O_4-ZIF).

The crystal structure of Co_3O_4 was studied by X-ray diffraction (Rigaku TTR-III). The morphology was analyzed by using a scanning electron microscope (SEM, JSM-6700F) and a transmission electron microscope (TEM, JEOL JEM-1200EX). Thermal gravimetric analysis (TGA) measurements were performed on a Netzsch STA 409 thermoanalyzer. The BET surface area measurements were performed with N_2 adsorption/desorption isotherms at 77 K on a NOVA 2200e analyzer.

2.2. Electrochemical Performance Measurements. The working electrodes were prepared by mixing 80 wt.% active substance (the prepared Co_3O_4), 10 wt.% carbon black, and 10 wt.% polytetrafluoroethylene with N-methyl-2-pyrrolidone; subsequently, the mixture was pressed onto a treated nickel foam which served as a current collector under a pressure of 10 MPa and dried at 70°C for 12 h. All electrochemical measurements were performed by an electrochemical workstation in a three-electrode system, with Ag/AgCl as the reference electrode, the Pt electrode as counter electrode, and the Co_3O_4 film electrode as the working electrode. The electrolyte used in this study was 1 M KOH solution.

3. Experimental Results and Discussion

3.1. Characterization of Precursors ZIF-67 and ZIF-8. Figure 1 shows the SEM images of precursors ZIF-8 and ZIF-67. SEM pictures reveal that the particles are nanocrystals in a polyhedral shape. The average diameter of ZIF-67 is about 90 nm. It can be clearly seen from the panoramic view (Figure 1(b)) that ZIF-8 sample contains uniform nanoparticles at 50 nm in diameter. The particle size of the ZIF-8 sample is much smaller than that of ZIF-67. Figure 2 gives the TGA curves in air of the precursors. As shown in Figure 2(a), the weight loss of ZIF-67 begins at about 250°C, indicating the onset of oxidation. While thermal decomposition of ZIF-8 begins at 350°C and there is a loss of 58% by weight, the thermal stability of ZIF-67 was slightly lower than that of ZIF-8.

3.2. X-Ray Diffraction Analysis. Figure 3 shows XRD chromatograms of Co_3O_4-TH and Co_3O_4-ZIF. It is obvious that the positions of the characteristic peaks in the two products are consistent. The peaks in curves of Co_3O_4-TH and Co_3O_4-ZIF are assigned to Co_3O_4 (JCPDS number 43-1003). No other peaks are observed in the XRD patterns. This suggests that the metal-organic framework does not exist after calcining, and there is no evidence of residual ZnO after washing. The average crystallite size calculated from the (311) peak using the Debye–Scherrer equation was 96 nm and 32 nm for Co_3O_4-TH and Co_3O_4-ZIF, respectively.

3.3. Morphology. TEM is employed in Figure 4 in order to observe the morphology and microstructure of the Co_3O_4 prepared by different methods. Figure 4(a) clearly implies that Co_3O_4 prepared through thermal decomposition of ZIF-67 is sphere-like product in large size. From Figure 4(a), it was apparent that the nanoparticles are seriously aggregated. Meanwhile, the particles are sphere-like structures with an average size about 100 nm. Jiang et al. reported the preparation of Co_3O_4 by converting cobalt oxide subunits in a Co-MOF ($Co_3(NDC)_3$, NDC = 2,6-naphthalene dicarboxylate) by pyrolysis in air. The prepared Co_3O_4 was agglomerated with an average size around 250 nm [25]. It is basically consistent with our experimental results.

It can be clearly seen from the panoramic view (Figure 4(b)) that the sample contains uniform and weak agglomerated Co_3O_4 nanoparticles with 30 nm in diameter. We know that the particle size of the Co_3O_4-ZIF sample is much smaller than that of Co_3O_4-TH. This suggests that the ZIF-8 framework may play an important role in preventing the migration and aggregation of cobalt precursor in the pores during the formation of Co_3O_4 upon heating.

3.4. Electrochemical Capacitor Property. Figures 5(a) and 5(b), respectively, show cyclic voltammograms (CV) curves of Co_3O_4-TH and Co_3O_4-ZIF electrodes in 1 M KOH solution at the scan rate of 20 mV s^{-1} within the potential range from 0 V to 0.4 V. Both curves exhibit apparent pseudocapacitance features with similar line-type in Figure 5, thereby demonstrating the capacitance that mainly derives from the rapid reversible redox of active materials within the potential range from 0 V to 0.4 V. Co_3O_4-ZIF electrode exhibits the larger current density compared with Co_3O_4-TH, thereby indicating that Co_3O_4-ZIF electrode possesses the higher specific capacitance. Besides, the peak currents increase with

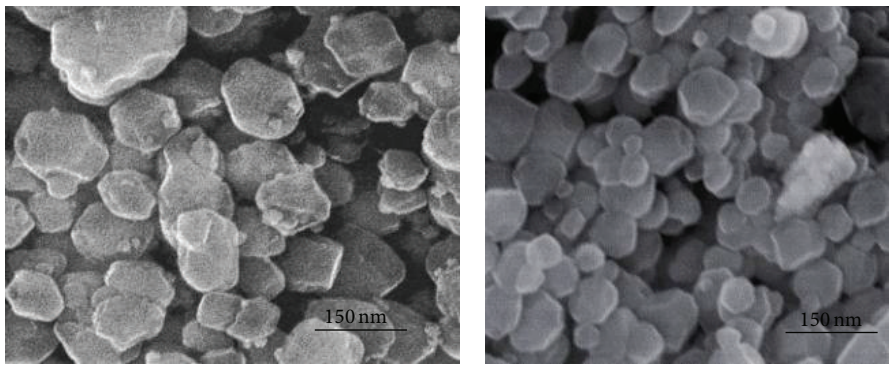

(a) (b)

Figure 1: SEM images of ZIF-67 (a) and ZIF-8 (b).

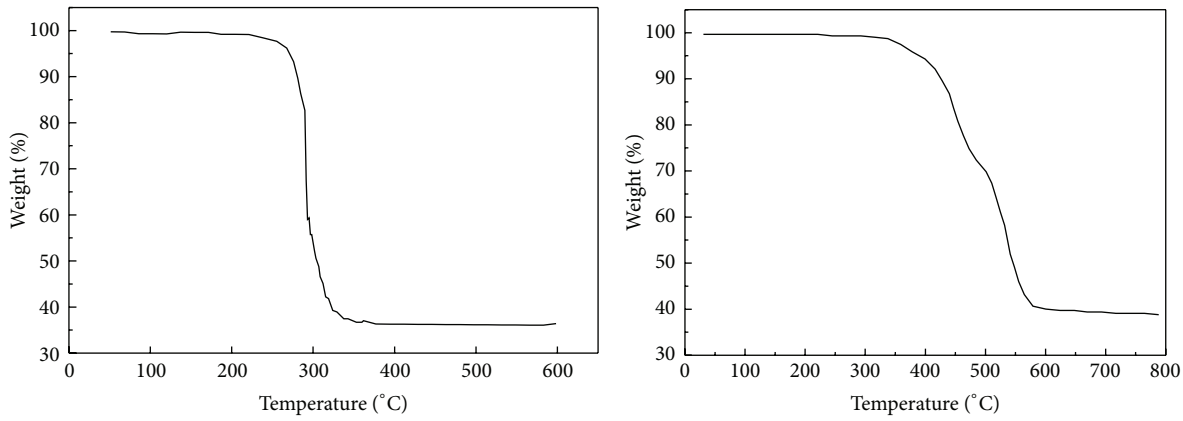

(a) (b)

Figure 2: TGA curves of ZIF-67 (a) and ZIF-8 (b).

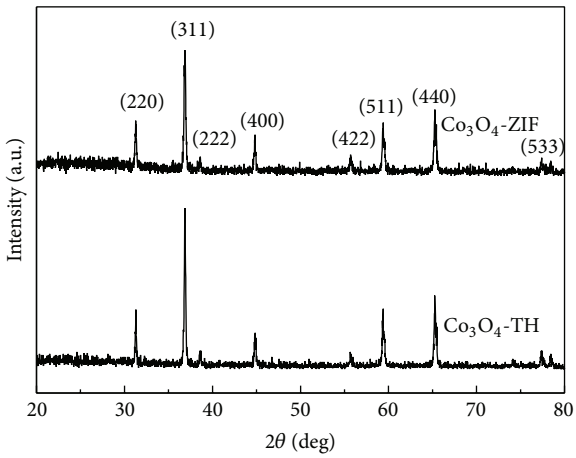

Figure 3: XRD chromatograms of Co_3O_4 samples prepared by two different methods.

the increase of the scan rate, indicating that rapid reversible redox reaction occurred among the electrode materials. The following redox reactions are considered to be responsible for the pseudocapacitance within the potential scanning range:

$$Co_3O_4 + H_2O + OH^- \leftrightharpoons 3CoOOH + e^- \quad (1)$$

Figure 6 shows constant current charge/discharge curves of Co_3O_4-TH and Co_3O_4-ZIF in 1 M KOH electrolyte at current density of 0.2 A g^{-1}. A nonlinear variation of potential versus time is observed during charge and discharge, thereby indicating that a pseudocapacitance performance arises from the electrochemical redox reaction occurring at Co_3O_4 electrode/electrolyte interface. The result is consistent with that from CV curves in Figure 5. Besides, the sudden potential drop, which represents the potential change because of the internal resistance, is observed [26]. The specific capacitance of the electrode can be calculated according to the following:

$$C = \frac{c}{m} = \frac{It}{m\Delta V}, \quad (2)$$

where I is the discharge current, t is the discharge time, ΔV is the potential range during discharge, and m is the mass of active material in the electrode. Figure 7 shows

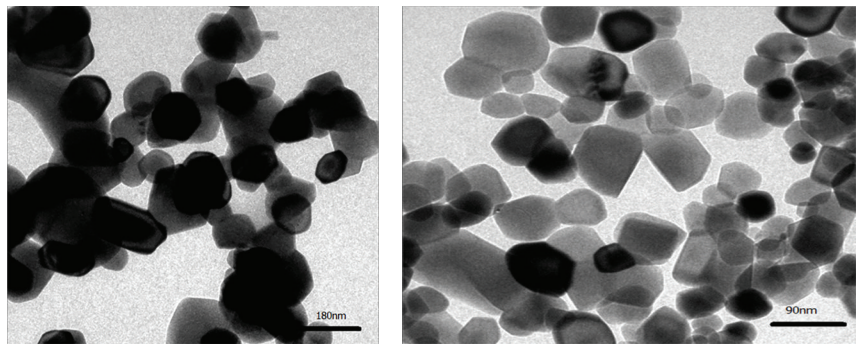

(a) (b)

Figure 4: TEM images of Co_3O_4-TH (a) and Co_3O_4-ZIF (b).

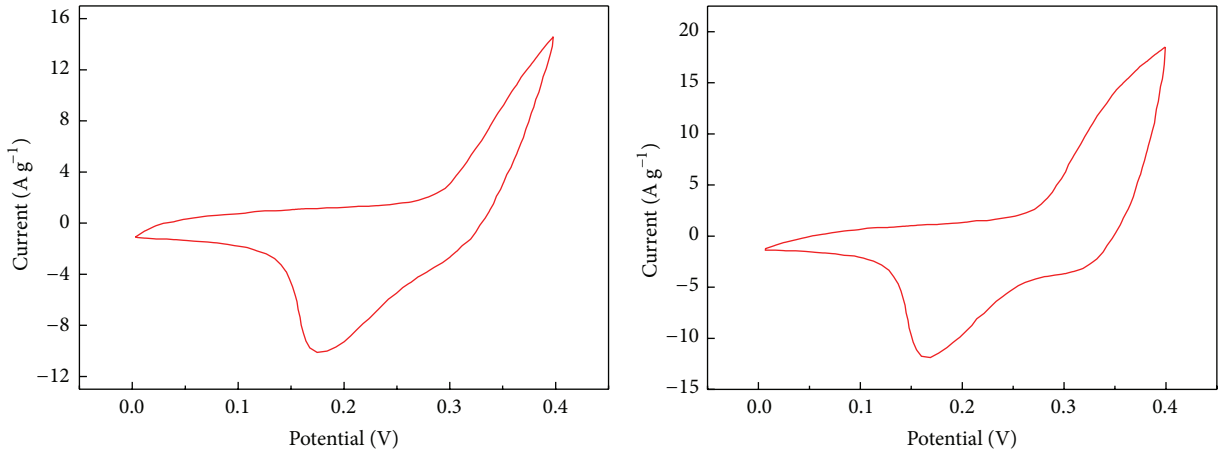

(a) (b)

Figure 5: Cyclic voltammograms curves of Co_3O_4-TH (a) and Co_3O_4-ZIF (b) electrodes.

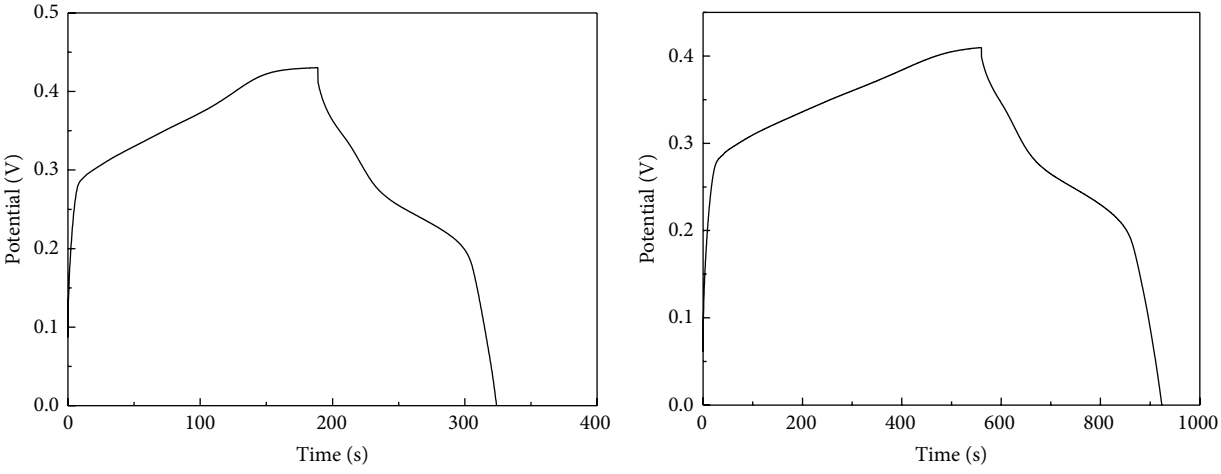

(a) (b)

Figure 6: Constant current charging and discharging curves of Co_3O_4-TH (a) and Co_3O_4-ZIF (b).

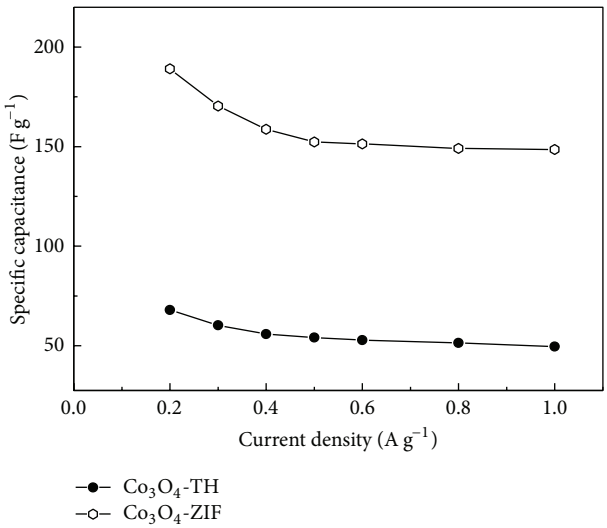

Figure 7: Relationship between the specific capacitance and the current density of Co_3O_4-TH and Co_3O_4-ZIF.

specific capacitance (C) of Co_3O_4 electrode at various specific currents (0.2, 0.3, 0.4, 0.5, 0.6, 0.8, and 1.0 A g^{-1}). The specific capacitance of Co_3O_4-TH is 67.9 F g^{-1}, while that of Co_3O_4-ZIF reaches 189.1 F g^{-1} when the current density is 0.2 A g^{-1}. We can see that the latter is obviously greater than the former in the specific capacitance. This value is comparable with that obtained from Co_3O_4 thin film (a maximum specific capacitance of 227 F g^{-1}) [10]. The Co_3O_4-ZIF electrode has the greater specific capacitance retention rate (78.5%) when the current density is increased from 0.2 to 1.0 A g^{-1}; similarly, its retention rate is higher than that (73.5%) of the Co_3O_4-TH electrode. The result indicates that the Co_3O_4-ZIF electrode is more suitable for fast discharging and charging.

The specific capacitance of Co_3O_4-ZIF is higher than that of Co_3O_4-TH. It can be proved from results of TEM that the particle size of Co_3O_4-ZIF is about 30 nm, while that of Co_3O_4-TH is about 100 nm. We can see that the latter is much larger than the former in the particle size. At the same time, the Co_3O_4-TH nanoparticles are seriously aggregated, and the aggregation of particles may decrease the surface area (the BET surface areas were calculated to be 11.32 m^2/g and 50.12 m^2/g for Co_3O_4-TH and Co_3O_4-ZIF, resp.). Based on this point, the former can fully contact with the electrolyte to greatly improve the specific capacitance. We can see that Co_3O_4 prepared by taking the ZIFs as the host can effectively control particle size and agglomeration and can effectively improve the specific capacitance.

4. Summary

The particle size of Co_3O_4-TH prepared through thermal decomposition of ZIF-67 as a precursor is relatively large, about 100 nm; meanwhile the Co_3O_4-TH particle shows agglomeration; the particle size of Co_3O_4-ZIF prepared by taking ZIF-8 as the host is generally small, about 30 nm, and the Co_3O_4-ZIF particle does not show agglomeration. From electrochemical property test results of two materials, the specific capacitance of Co_3O_4-ZIF is obviously greater than that of Co_3O_4-TH. The specific capacitance of the former reaches 189.1 F g^{-1} at the current density of 0.2 A g^{-1}. This suggests that the ZIF-8 framework may play an important role in preventing the migration and aggregation of cobalt precursor in the pores during the formation of Co_3O_4 upon heating. The Co_3O_4 can fully contact with the electrolyte, greatly improving the specific capacitance.

Conflict of Interests

The authors declare that there is no conflict of interests regarding the publication of this paper.

Acknowledgments

This work was supported by the Fundamental Research Funds for the Central Universities (2012QNA05), the National Natural Science Foundation of China (Project no. 51304198), and the Natural Science Foundation of Jiangsu Province (Project no. BK2014028-08).

References

[1] M. H. Ervin, L. T. Le, and W. Y. Lee, "Inkjet-printed flexible graphene-based supercapacitor," *Electrochimica Acta*, vol. 147, pp. 610–616, 2014.

[2] M. Mohammedi, O. Kraa, M. Becherif et al., "Fuzzy logic and passivity-based controller applied to electric vehicle using fuel cell and supercapacitors hybrid source," *Energy Procedia*, vol. 50, pp. 619–626, 2014.

[3] Z. Song, J. Li, X. Han et al., "Multi-objective optimization of a semi-active battery/supercapacitor energy storage system for electric vehicles," *Applied Energy*, vol. 135, pp. 212–224, 2014.

[4] L. G. H. Staaf, P. Lundgren, and P. Enoksson, "Present and future supercapacitor carbon electrode materials for improved energy storage used in intelligent wireless sensor systems," *Nano Energy*, vol. 9, pp. 128–141, 2014.

[5] H. Yang and Y. Zhang, "A study of supercapacitor charge redistribution for applications in environmentally powered wireless sensor nodes," *Journal of Power Sources*, vol. 273, pp. 223–236, 2015.

[6] V. Yuhimenko, M. Averbukh, G. Agranovich, and A. Kuperman, "Dynamics of supercapacitor bank with uncontrolled active balancer for engine starting," *Energy Conversion and Management*, vol. 88, pp. 106–112, 2014.

[7] Y. Huang, C. Chen, C. An et al., "Synthesis of cobalt based complexes and conversion to Co_3O_4 nanoparticles as a high performance anode for lithium ion battery," *Electrochimica Acta*, vol. 145, pp. 34–39, 2014.

[8] J. H. Kwak, Y.-W. Lee, and J. H. Bang, "Supercapacitor electrode with an ultrahigh Co_3O_4 loading for a high areal capacitance," *Materials Letters*, vol. 110, pp. 237–240, 2013.

[9] Y. Li, K. Huang, S. Liu, Z. Yao, and S. Zhuang, "Meso-macroporous Co_3O_4 electrode prepared by polystyrene spheres and carbowax templates for supercapacitors," *Journal of Solid State Electrochemistry*, vol. 15, no. 3, pp. 587–592, 2011.

[10] Y. Li, K. Huang, Z. Yao, S. Liu, and X. Qing, "Co_3O_4 thin film prepared by a chemical bath deposition for electrochemical

capacitors," *Electrochimica Acta*, vol. 56, no. 5, pp. 2140–2144, 2011.

[11] W. Wang, Y. Li, R. Zhang, D. He, H. Liu, and S. Liao, "Metal-organic framework as a host for synthesis of nanoscale Co_3O_4 as an active catalyst for CO oxidation," *Catalysis Communications*, vol. 12, no. 10, pp. 875–879, 2011.

[12] H. Xu, L. Gao, Q. Zhang et al., "Preparation method of Co_3O_4 nanoparticles using degreasing cotton and their electrochemical performances in supercapacitors," *Journal of Nanomaterials*, vol. 2014, Article ID 723057, 9 pages, 2014.

[13] Z. Hasan and S. H. Jhung, "Removal of hazardous organics from water using metal-organic frameworks (MOFs): plausible mechanisms for selective adsorptions," *Journal of Hazardous Materials*, vol. 283, pp. 329–339, 2015.

[14] J. Kim, S. Yeo, J.-D. Jeon, and S.-Y. Kwak, "Enhancement of hydrogen storage capacity and hydrostability of metal–organic frameworks (MOFs) with surface-loaded platinum nanoparticles and carbon black," *Microporous and Mesoporous Materials*, vol. 202, pp. 8–15, 2015.

[15] S. Y. Lim, J. Choi, H.-Y. Kim et al., "New CO_2 separation membranes containing gas-selective Cu-MOFs," *Journal of Membrane Science*, vol. 467, pp. 67–72, 2014.

[16] D. Zhao, X. Wan, H. Song, L. Hao, Y. Su, and Y. Lv, "Metal-organic frameworks (MOFs) combined with ZnO quantum dots as a fluorescent sensing platform for phosphate," *Sensors and Actuators B: Chemical*, vol. 197, pp. 50–57, 2014.

[17] R. K. Bhakta, J. L. Herberg, B. Jacobs et al., "Metal-organic frameworks as templates for nanoscale $NaAlH_4$," *Journal of the American Chemical Society*, vol. 131, no. 37, pp. 13198–13199, 2009.

[18] M. Müller, S. Hermes, K. Kähler, M. W. E. van den Berg, M. Muhler, and R. A. Fischer, "Loading of MOF-5 with Cu and ZnO nanoparticles by gas-phase infiltration with organometallic precursors: properties of Cu/ZnO@MOF-5 as catalyst for methanol synthesis," *Chemistry of Materials*, vol. 20, no. 14, pp. 4576–4587, 2008.

[19] M. Müller, X. Zhang, Y. Wang, and R. A. Fischer, "Nanometer-sized titania hosted inside MOF-5," *Chemical Communications*, vol. 7, no. 1, pp. 119–121, 2009.

[20] D. Ge and H. K. Lee, "Water stability of zeolite imidazolate framework 8 and application to porous membrane-protected micro-solid-phase extraction of polycyclic aromatic hydrocarbons from environmental water samples," *Journal of Chromatography A*, vol. 1218, no. 47, pp. 8490–8495, 2011.

[21] J. A. Thompson, K. W. Chapman, W. J. Koros, C. W. Jones, and S. Nair, "Sonication-induced Ostwald ripening of ZIF-8 nanoparticles and formation of ZIF-8/polymer composite membranes," *Microporous and Mesoporous Materials*, vol. 158, pp. 292–299, 2012.

[22] G. Xu, J. Yao, K. Wang et al., "Preparation of ZIF-8 membranes supported on ceramic hollow fibers from a concentrated synthesis gel," *Journal of Membrane Science*, vol. 385-386, no. 1, pp. 187–193, 2011.

[23] J. Yao, L. Li, W. H. Benjamin Wong, C. Tan, D. Dong, and H. Wang, "Formation of ZIF-8 membranes and crystals in a diluted aqueous solution," *Materials Chemistry and Physics*, vol. 139, no. 2-3, pp. 1003–1008, 2013.

[24] J. Qian, F. Sun, and L. Qin, "Hydrothermal synthesis of zeolitic imidazolate framework-67 (ZIF-67) nanocrystals," *Materials Letters*, vol. 82, pp. 220–223, 2012.

[25] H.-L. Jiang, N. Tsumori, and Q. Xu, "A series of (6,6)-connected porous lanthanide-organic framework enantiomers with high thermostability and exposed metal sites: scalable syntheses, structures, and sorption properties," *Inorganic Chemistry*, vol. 49, no. 21, pp. 10001–10006, 2010.

[26] Y. Li, K. Huang, D. Zeng, S. Liu, and Z. Yao, "RuO_2/Co_3O_4 thin films prepared by spray pyrolysis technique for supercapacitors," *Journal of Solid State Electrochemistry*, vol. 14, no. 7, pp. 1205–1211, 2010.